The First Symposium on Carbon Ultimate Utilization Technologies for
the Global Environment (CUUTE-1)
Ed. by T. Sando, M. Kitatsugi and J. Ryo
The Iron and Steel Institute of Japan, 2021

Decarbonisation of carbon-intensive industries (Iron and Steel Industries) through Power to gas and Oxy-fuel combustion

Manuel Bailera[1,2*], Takao Nakagaki[3], Irmela Kofler[4], Luis M. Romeo[2]

[1]*Graduate School of Creative Science and Engineering, Waseda University, Okubo, Shinjuku-ku, 169-8555 Tokyo, Japan*
[2]*Escuela de Ingeniería y Arquitectura, Universidad de Zaragoza, Campus Río Ebro, María de Luna 3, 50018 Zaragoza, Spain*
[3]*Department of Modern Mechanical Engineering, Waseda University, Tokyo, Japan*
[4]*K1-MET GmbH, Stahlstraße 14, 4020 Linz, Austria*
*Corresponding autor: *mbailera@unizar.es*

Keywords: *Iron and steel, Power to Gas, Rist diagram, Operating line, Oxy-fuel combustion, Blast furnace, CO_2 mitigation, Methanation, Carbon recycling*

1. Introduction

The potential contribution of carbon capture and utilization to the global warming mitigation challenge has shown to be very limited when compared to geological storage or electrification [1,2]. If we talk in particular about e-fuels (e.g., hydrogen from renewables and synthetic methane), the electricity-to-useful-power efficiencies range from roughly 10% to 35%, meaning that energy requirements are 2–14 times higher than for direct electrification [2].

However, some of the most energy- and carbon-intensive sectors worldwide face limitations when applying electrification. In some cases this is because the requirement of high-temperature heat above 400 ºC (e.g., glass, cement) and others because the nature of the process itself (e.g., ironmaking, long-distance aviation and shipping) [2].

Renewable hydrogen and synthetic fuels can overcome this barriers, delivering the same service at lower costs than the other CO_2 abatement alternatives, so they should be targeted on these industries from an economic and carbon-neutrality perspective [1,2]. Furthermore, given the substantial size of the mentioned sectors, the application of e-fuels within them should be prioritized [2].

2. DISIPO project

In this framework, the DISIPO project (*Decarbonisation of carbon-intensive industries (Iron and Steel Industries) through Power to gas and Oxy-fuel combustion*) presents a novel concept that combines Power to Gas (PtG) and oxy-fuel combustion to decarbonise the ironmaking process (**Fig. 1**) [3]. PtG technology consumes renewable electricity to produce H_2 and O_2 through water electrolysis. The O_2 allows reducing the energy consumption of the air separation unit that feeds the oxy-fuel blast furnace, while H_2 is combined with the CO_2-rich blast furnace gas to produce synthetic natural gas (SNG) via methanation [3,4]. This SNG is used as reducing agent in the blast furnace, keeping carbon in a closed loop [5].

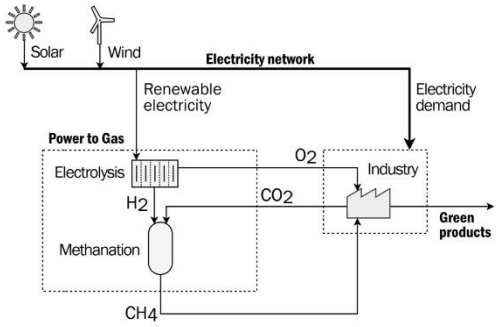

Fig. 1 Conceptual scheme of proposed concept

The project is divided in several work packages, aiming (i) to design, simulate and optimize the integrated layout of the novel proposed concept, (ii) to assess the maximum feasible CO_2 abatement under advanced control strategies adapted to the availability of the renewable energy resource, and (iii) to compare the proposed concept with conventional CCS under life-cycle analysis and economic assessment.

The first results of the project are presented in this paper. These cover the Rist diagram model and the operating line of an oxygen blast furnace (OBF) with SNG injection.

3. Revisiting the Rist diagram

The Rist diagram is named so in reference to its author, who elaborated a model for predicting changes in blast furnaces when the operating conditions are modified. The model is based on the graphical representation of carbon, oxygen, and hydrogen balances through an operation line (**Eq. 1**), which depicts the participation of these elements in the formation of the reducing gas and its later utilization [6]. Here, μ is the number of moles of reducing gas required for the production of 1 atom of Fe (CO and H_2), and Y_E represents the moles of H_2 and O atoms (from sources other than iron oxides) that contribute to the formation of the reducing gas [7].

$$Y = \mu \cdot X + Y_E \quad (1)$$

The operating line is obtained by computing two points denoted as W and P. The former represents the equilibrium between gases and solids reached in a zone of pure wüstite and corresponding to the chemical reserve zone. The latter is imposed by the energy balance in the blast furnace.

The original model is thoroughly explained in a series of papers that progressively deeps into the topic [6–10]. However, some of the most important parts were not written in English, and a paper summarizing the general model was not available. As a result, relevant aspects of his work are sometimes no widely known. Such is the case that some authors claim to modify Rist diagram to include the H_2 contribution [11,12], when in fact this was already took into account by Rist. For these reasons, we decided to revisit his original work, during which we made a number of additions and corrections (e.g., detailed equation for computing the lack of chemical ideality, model for computing the heat of decomposition of coal, or correction on the sensible heat of the slag).

3.1 Model validation

The Rist model has been validated with data from a conventional blast furnace [13]. The heat removed by the staves is 744.8 MJ/THM [13], the temperature of the chemical reserve zone is 897 ºC, and the chemical efficiency is assumed 92% [14]. Results show an error around or below 5% (**Table 1**). The degree of oxidation of the top gas in the simulation is 46.4% and in the reference data is 45.6% (error of 1.7%).

Table 1 Comparison of model and reference (conventional BF).

Stream (kg/THM)	Model	Reference[13]	Error (%)
Sintered ore	1250	1250	(Input data)
Ore pellets	342	342	(Input data)
Aux. material	15	15	(Input data)
Coke	387	380	+1.8
Pulverized coal	112	112	(Input data)
Hot air	1420	1346	+5.5
Moisture	29	28	+5.5
Oxygen	35	35	(Input data)
Hot metal	1002	1002	-0.1
Slag	281	279	+0.7
BFG	2308	2225	+3.7

4. Operating line of an OBF with SNG gas injection

The conceptual scheme of the oxygen blast furnace is depicted in **Fig. 2**. It includes Top gas recycling (TGR) to use the CO-rich gas obtained after the carbon capture stage. The base case is inspired on the work of Jin et al. [15]. The heat removed is 250 MJ/THM, the temperature of the chemical reserve zone is 984 ºC, and the chemical efficiency is 94%. The CO_2 emissions are 946 kg/THM.

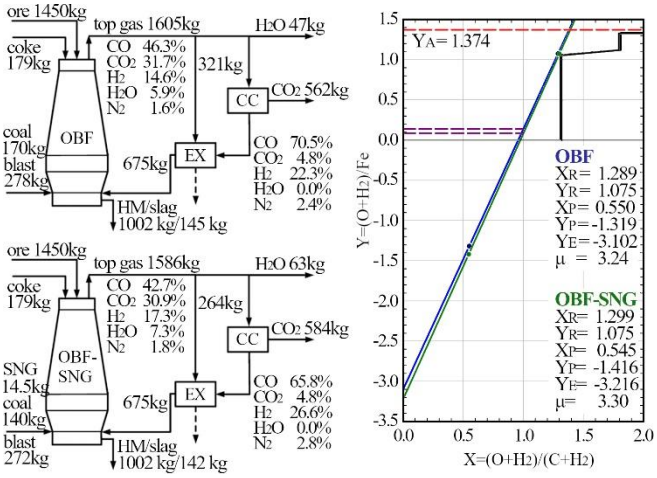

Fig. 2 OBF (base case) and OBF with SNG injection.

In the case of OBF with SNG injection, we assume 100 MW PtG capacity for a 280 THM/h OBF. This means a SNG production of 14.5 kg/THM (40 kg of CO_2 in closed loop). To keep injecting 675 kg of CO-rich gas, the recirculation ratio increases from 80% to 83%. The chemical reserve zone is at 938 ºC. The CO_2 emissions are 674 kg/THM, and the coal is reduced by 17.6%. The energy penalization of CO_2 avoidance is 4.7 MJ/kg_{CO2}, which is in the range of conventional amine carbon capture, with the benefit of reducing coal consumption.

Acknowledgement

The DISIPO project received funding from the European Union's Horizon 2020 research and innovation programme under the Marie Sklodowska-Curie grant No 887077.

REFERENCES

1) Mac Dowell, N., Fennell, P. S., Shah, N. & Maitland, G. C. Nat. Clim. Chang. 7 (2017), 243–249. https://doi.org/10.1038/nclimate3231.
2) Ueckerdt, F. et al. Nat. Clim. Chang. 11 (2021), 384–393. https://doi.org/10.1038/s41558-021-01032-7.
3) Bailera, M., Lisbona, P., Peña, B. & Romeo, L. M. J. CO2 Util. 46 (2021), 101456. https://doi.org/10.1016/j.jcou.2021.101456.
4) Bailera, M., Lisbona, P. & Romeo, L. M. Int. J. Hydrogen Energy 40 (2015), https://doi.org/10.1016/j.ijhydene.2015.06.074.
5) Romeo, L. M. & Bailera, M. J. CO2 Util. 39 (2020), 101174. https://doi.org/10.1016/j.jcou.2020.101174.
6) Rist, A. & Meysson, N. Jom 19 (1967), 50–59. https://doi.org/10.1007/bf03378564.
7) Meysson, N., Weber, J. & Rist, A. Rev. Métallurgie 61 (1964), 623–633. https://doi.org/10.1051/metal/196461070623.
8) Rist, A. & Meysson, N. Rev. Metall. 62 (1965), 995–1040. https://doi.org/10.1051/metal/196562110995.
9) Rist, A. & Meysson, N. Rev. Métallurgie 61 (1964), 121–146. https://doi.org/10.1051/metal/196461020121.
10) Kundrat, D. M., Miwa, T. & Rist, A. Metall. Trans. B 22B (1991), 363–383. https://doi.org/10.1007/bf02651235.
11) Tang, J. et al. J. Clean. Prod. 278 (2021), 123191. https://doi.org/10.1016/j.jclepro.2020.123191.
12) Zhan, W. L., Wu, K., He, Z. J., Liu. Iron Steel Res. Int. 22 (2015), 1078–1084. https://doi.org/10.1016/s1006-706x(15)30115-1.
13) Suzuki, K., Hayashi, K., Kuribara, K., Nakagaki, T. & Kasahara, S. ISIJ Int. 55 (2015), 340–347. doi.org/10.2355/isijinternational.55.340.
14) Hisashige, S., Nakagaki, T. & Yamamoto, T. ISIJ Int. 59 (2019), 598–606. https://doi.org/10.2355/isijinternational.isijint-2018-355.
15) Jin, P. et al. Steel Res. Int. 87 (2016), 320–329. https://doi.org/10.1002/srin.201500054.